arXiv:1410.2406v1 [cond-mat.str-el] 9 Oct 2014

Generation of localized magnetic moments in the charge-density-wave state

R.S. Akzyanov[1,2,3] and A.V. Rozhkov[1,2]

[1] *Moscow Institute for Physics and Technology (State University), 141700 Moscow Region, Russia*
[2] *Institute for Theoretical and Applied Electrodynamics, Russian Academy of Sciences, 125412 Moscow, Russia*
[3] *All-Russia Research Institute of Automatics, Moscow, 127055 Russia*

We propose a mechanism explaining the generation of localized magnetic moments in charge-density-wave compounds. Our model Hamiltonian describes an Anderson impurity placed in a host material exhibiting the charge-density wave. There is a region of the model's parameter space, where even weak Coulomb repulsion on the impurity site is able to localize the magnetic moment on the impurity. The phase diagram of a single impurity at $T = 0$ is mapped. To establish the connection with experiment thermodynamic properties of a random impurity ensemble is studied. Magnetic susceptibility of the ensemble diverges at low temperature; heat capacity as a function of the magnetic field demonstrates pronounced low field peak. Both features are consistent with experiments on orthorhombic TaS_3 and blue bronze.

PACS numbers: 71.10.Pm, 03.67.Lx, 74.45.+c

I. INTRODUCTION

Study of coexistence and competition between different types of order is a recurrent theme of the modern condensed matter research, both theoretical and experimental. In this paper we discuss a particular example of such coexistence. There is significant experimental evidence that several charge-density wave (CDW) materials (orthorhombic TaS_3, Ref. 1,2; blue bronze Ref. 3; non-magnetic tritellurides YTe_3 and $LaTe_3$, Ref. 4) show unusual sensitivity to the magnetic field at low temperatures. For example, magnetic susceptibility of o-TaS_3 is temperature-independent in a broad range of temperatures, both above and below its CDW transition temperature $T_{\rm CDW}$=218 K (see Fig.1 of Ref. 1). However, below $\sim$60 K the susceptibility begins to grow quickly as the temperature decreases. Experimental investigation of low-temperature magnetic and thermodynamic properties concluded[1] that such a behavior is consistent with the assumption that a disordered ensemble of localized magnetic moments undergoes a transition into a glass state.

This magnetic glass is quite unexpected (non-magnetic glass[6] induced by the CDW pinning is, of course, possible, but it has little relevance to the issue under consideration). Theoretically, the CDW magnetic properties are believed to be trivial: due to the gap in the electron spectrum, at temperatures significantly below $T_{\rm CDW}$ electronic contribution to the susceptibility vanishes. How localized magnetic moments can emerge under such circumstances?

In this paper we propose a mechanism, which may explain the origin of these magnetic moments. We will study an impurity inside a CDW compound. Assuming weak electron repulsion at the impurity site, we find a parameter regime where exactly one electron resides on that site. Spins of such electrons are responsible for low-temperature magnetism of the CDW material.

Our mechanism is quite generic, and does not impose special restrictions on the dimensionality of the Hamiltonian, band structure, and other model details. However, the low-temperature magnetism of an CDW compound is by no means a universal feature: if the system parameters are outside of the required range, the magnetic response is completely trivial. Of course, a particular material may enter this regime either by luck, or by intelligent design of a material scientist.

Our paper is organized as follows. In Sec. II we introduce our model Hamiltonian. Generation of the magnetic moment on a single impurity is discussed in Sec. III. Thermodynamic properties of an ensemble of these impurities is investigated in Sec. IV. The discussion are presented in Sec. V. We conclude in Sec. VI.

II. MODEL

We study a single Anderson impurity, which is located inside the host material with CDW ground state. The model's Hamiltonian H is equal to

$$H = H_{\rm F} + H_{\rm imp} + H_{\rm hop}, \tag{1}$$

where Fröhlich Hamiltonian $H_{\rm F}$, Anderson Hamiltonian $H_{\rm imp}$, and hybridization Hamiltonian $H_{\rm hop}$ are defined as follows:

$$H_{\rm F} = \sum_{\mathbf{k}\sigma} \left(\epsilon_{\mathbf{k}} a^\dagger_{1,\mathbf{k}\sigma} a_{1,\mathbf{k}\sigma} - \epsilon_{\mathbf{k}} a^\dagger_{2,\mathbf{k}\sigma} a_{2,\mathbf{k}\sigma} \right) + \sum_{\mathbf{k}\sigma} \Delta \left(e^{i\phi} a^\dagger_{1,\mathbf{k}\sigma} a_{2,\mathbf{k}\sigma} + \text{H.c.} \right), \tag{2}$$

$$H_{\rm imp} = \sum_{\sigma} (-\epsilon_0) d^\dagger_\sigma d_\sigma + U d^\dagger_\uparrow d_\uparrow d^\dagger_\downarrow d_\downarrow, \tag{3}$$

$$H_{\rm hop} = \sum_{\mathbf{k}\sigma} t (a^\dagger_{1,\mathbf{k}\sigma} + a^\dagger_{2,\mathbf{k}\sigma}) d_\sigma + \text{H.c.} \tag{4}$$

This model describes two bands of electrons with perfect nesting. The dispersion of the first band is $\epsilon_{\mathbf{k}}$, the dispersion in the second band is $-\epsilon_{\mathbf{k}}$. Band electron creation

operators are $a^\dagger_{\alpha,\mathbf{k}\sigma}$, where $\alpha = 1, 2$, is the band index, $\mathbf{k}$ and σ are momentum and spin of the electron.

The CDW phase is characterized by a finite value of the order parameter Δ, which we assume to be real and positive. The quantity ϕ in Eq. (2) equals to CDW phase

$$\phi = \mathbf{K}_\mathrm{n} \cdot \mathbf{R}_\mathrm{imp} \tag{5}$$

at the location of the impurity $\mathbf{R}_\mathrm{imp}$. (In this equation $\mathbf{K}_\mathrm{n}$ is the nesting vector of the Fermi surface.)

Operator $d^\dagger_\sigma$ creates an electron at the impurity site. Single-electron energy at the impurity is equal to $-\epsilon_0$. The hybridization amplitude between the impurity state and the bands is t. The electron-electron interaction at the impurity site is $U > 0$. In this paper we assume that U is small:

$$U \ll \Delta. \tag{6}$$

This is a necessary condition for the use of the perturbation theory in powers of the interaction.

III. SINGLE-IMPURITY PROPERTIES

First, let us briefly discuss the properties of our model in the "high temperature" regime, $T > T_\mathrm{CDW}$, $\Delta(T) = 0$. When U is small, and the temperature is high, the Kondo correlations at the impurity site are negligible: combining inequality (6) and inequality $T_\mathrm{K} \ll U$, we derive

$$T_\mathrm{K} \ll U \ll \Delta(0) \sim T_\mathrm{CDW} < T \tag{7}$$

for this regime. Consequently, the interaction at the impurity site can be treated perturbatively. Thus, above the transition into the ordered state our model describes electrons experiencing potential scattering off the impurity. When we generalize our model to include many impurities randomly placed in the sample, we should recover the usual phenomenology of a metal with disorder.

The low temperature behavior of the model is much less trivial, as we will see below. Experimentally, the magnetic susceptibility starts to diverge when the temperature is significantly smaller than T_CDW. Thus, we will study the regime

$$T \ll T_\mathrm{CDW}. \tag{8}$$

In this limit the CDW order parameter is independent of temperature, and it is permissible to use its zero-temperature value for calculations.

For weak interaction, Eq. (6), perturbation theory is allowed. To apply the perturbation theory we need to find the eigenstates and eigenenergies of the unperturbed Hamiltonian. The unperturbed Hamiltonian is given by Eq. (1) in which we put $U = 0$. It can be diagonalized straightforwardly. It is convenient to introduce a set of creation operators corresponding to eigenstates with energy E

$$A_E = \delta_E d^\dagger + \sum_\mathbf{k} \beta_{E\mathbf{k}} a^\dagger_{1,\mathbf{k}} + \gamma_{E\mathbf{k}} a^\dagger_{2,\mathbf{k}}, \tag{9}$$

where A_E satisfies the equation:

$$[H, A_E] = E A_E. \tag{10}$$

Here δ_E, $\beta_{E\mathbf{k}}$, and $\gamma_{E\mathbf{k}}$ are c-number coefficients. We do not show the spin index explicitly since the $U = 0$ Hamiltonian can be split into two identical Hamiltonians for two spin projections.

A. Subgap bound state

Equation (10) is equivalent to a system of linear equations on coefficients δ_E, $\beta_{E\mathbf{k}}$, and $\gamma_{E\mathbf{k}}$. For this system to have a solution, E must satisfy the following equation:

$$E + \epsilon_0 - 2t^2 (E + |\Delta| \cos\phi) \sum_\mathbf{k} \frac{1}{E^2 - \epsilon^2_\mathbf{k} - |\Delta|^2} = 0. \tag{11}$$

This equation may have a subgap solution $|E_0| < \Delta$:

$$E_0 = -\epsilon_0 - \Gamma \frac{E_0 + |\Delta| \cos\phi}{\sqrt{\Delta^2 - E_0^2}}, \tag{12}$$

$$\text{where } \Gamma = 2\pi t^2 \rho_\mathrm{n} V \tag{13}$$

is the width of the impurity level [ρ_n is the density of states at the Fermi energy in metallic state, V is the sample volume]. There is no more than one subgap solution. It corresponds to an electron bound to the impurity site. Energy E_0 is zero if

$$\epsilon_0 = -\Gamma \cos\phi. \tag{14}$$

When the order parameter is large ($\Delta \gg \epsilon_0, \Gamma$), Eq. (12) may be solved approximately:

$$E_0 \approx -\epsilon_0 - \Gamma \cos\phi. \tag{15}$$

The energy of the bound state depends on the local value of ϕ. The density of extended states, which will be evaluated below, is also sensitive to ϕ. These facts are not surprising: the quantum tunneling between the impurity and the bands is sensitive to the value of local charge density, which is proportional to $\exp(i\phi)$.

B. Density of extended states

The presence of the impurity not only generates the bound state, but also affects the density of states in the bulk. For $|E| > \Delta$ the density of extended states can be calculated with the help of the following trick[7]. All eigenenergies are solutions of Eq. (11). Thus, the density of states is equal to the "density of zeros" for the function:

$$\begin{aligned} F(E) &= -\epsilon_0 - E \\ &+ 2t^2 (E + \Delta\cos\phi) \sum_\mathbf{k} \frac{1}{E^2 - \epsilon^2_\mathbf{k} - \Delta^2}. \end{aligned} \tag{16}$$

However, this function has not only zeros, but poles as well. It is convenient to define the following polynomial:

$$P(E) = F(E) \prod_{\mathbf{k}} (E^2 - \epsilon_{\mathbf{k}}^2 - \Delta^2). \quad (17)$$

This polynomial has identical set of roots as $F(E)$, and no singularities. Thus, the density of states $\rho(E)$ is equal to

$$\rho(E) = \frac{1}{\pi} \lim_{\omega \to +0} \frac{d}{dE} \mathrm{Im} \left[\ln P(E + i\omega) \right]. \quad (18)$$

To prove this formula it is enough to notice that its right-hand side is a sum of delta-functions $\sum_n \delta(E - E_n)$, where E_n are the roots of $P(E)$, and, consequently, of $F(E)$.

The right-hand side of Eq. (18) can be calculated in the thermodynamic limit. For finite $\omega > 0$ one can replace the sum in the definition of F, Eq. (16), by the integral, which can be evaluated. Finally, we obtain

$$\rho(E) = \rho_0(E) + \frac{1}{\pi} \frac{d}{dE} \arctan \frac{\Gamma(E + \Delta \cos\phi)}{(\epsilon_0 + E)\sqrt{E^2 - \Delta^2}}, \quad (19)$$

$$\rho_0(E) = \rho_{\mathrm{n}} \frac{E}{\sqrt{E^2 - \Delta^2}}. \quad (20)$$

Here ρ_0 is the usual BCS-like density of states. The density of states $\rho(E)$ will be used below to calculate the average filling fraction of the impurity site.

C. Unperturbed many-electron states

Now, when we have finished describing the single-electron states of the $U = 0$ Hamiltonian, we must construct a set of many-electron states, which will be the starting point of perturbation theory calculations.

It is assumed that at low temperature all negative-energy extended states are occupied, and positive-energy extended states are empty. However, the low-lying subgap states may be empty or occupied, depending on different conditions (temperature, interaction, magnetic field). To account for these possibilities we will keep track of four many-electron states $|N_\uparrow, N_\downarrow\rangle$, where numbers

$$N_\sigma = 0 \text{ or } 1 \quad (21)$$

show how many electrons with spin σ sit at the impurity bound state. The energy of $|N_\uparrow, N_\downarrow\rangle$ equals to:

$$E = \sum_\sigma E_\sigma, \quad (22)$$

$$E_\sigma = E_0 N_\sigma + \int \bar{E} \rho(\bar{E}) \Theta(-\Delta - \bar{E}) d\bar{E}. \quad (23)$$

Here $\Theta(x)$ is the step-function.

D. Filling fraction of the impurity site

To apply the perturbation theory, we will need the following matrix element:

$$\langle n_\sigma \rangle = \langle N_\uparrow, N_\downarrow | \, d_\sigma^\dagger d_\sigma \, | N_\uparrow, N_\downarrow \rangle . \quad (24)$$

Since the non-interacting Hamiltonian does not couple different spin projections, $\langle n_\sigma \rangle$ depends on N_σ, but not on $N_{-\sigma}$. Physically, $\langle n_\sigma \rangle$ is equal to probability of finding electron with spin σ on the impurity. Note that this probability is not equal to N_σ.

To calculate $\langle n_\sigma \rangle$ it is convenient to use the Hellmann-Feynman theorem, which states that, if $|\psi_n(\lambda)\rangle$ is an eigenstate of a Hamiltonian $H = H(\lambda)$:

$$H(\lambda) \, |\psi_n(\lambda)\rangle = E_n(\lambda) \, |\psi_n(\lambda)\rangle , \quad (25)$$

where λ is some parameter, then

$$\frac{\partial E_n}{\partial \lambda} = \langle \psi_n | \frac{\partial H}{\partial \lambda} | \psi_n \rangle . \quad (26)$$

Using the latter equation, we can write

$$\langle n_\sigma \rangle = -\frac{\partial E_\sigma}{\partial \epsilon_0}, \quad (27)$$

where E_σ is determined by Eq. (23). The formula for $\langle n_\sigma \rangle$ has two terms:

$$\langle n_\sigma \rangle = n_0 + n_1 N_\sigma, \quad (28)$$

$$n_0 = \int \bar{E} \frac{\partial \rho(\bar{E})}{\partial \epsilon_0} \Theta(-\Delta - \bar{E}) d\bar{E}, \quad (29)$$

$$n_1 = \frac{\partial E_0}{\partial \epsilon_0}. \quad (30)$$

The quantity n_0, Eq. (29) is independent of N_σ, and identical for both spin projections. It is always non-zero as long as the impurity level has finite hybridization with the band electrons. General analytic calculations for n_0 are quite cumbersome, however, some simple equations can be obtained in the limit $\epsilon_0 \ll \Delta$. When $\phi = \frac{\pi}{2}$, for arbitrary Γ the following relation can be derived:

$$n_0(\phi = \frac{\pi}{2}) = \frac{1}{2} \frac{\Gamma}{\Gamma + \Delta}. \quad (31)$$

If we assume further that $\Gamma < \Delta$, then

$$n_0(\phi = 0) \simeq \frac{\Gamma}{\Delta} (\frac{1}{2} - \frac{1}{\pi}). \quad (32)$$

The second term, $N_\sigma n_1$, obviously depends on the occupation of the bound state level by an electron with spin σ. Using Eq. (12) we derive

$$n_1 = \frac{(\Delta^2 - E_0^2)^{\frac{3}{2}}}{(\Delta^2 - E_0^2)^{\frac{3}{2}} + \Gamma \Delta (\Delta + E_0 \cos\phi)}. \quad (33)$$

Both n_0 and n_1 are plotted in Fig. 1. Examining this figure one can notice that, if $E_0 < 0$ and $\epsilon_0, \Gamma < \Delta$, then the contribution of zone electrons n_0 is much smaller than contribution of the localized electrons n_1.

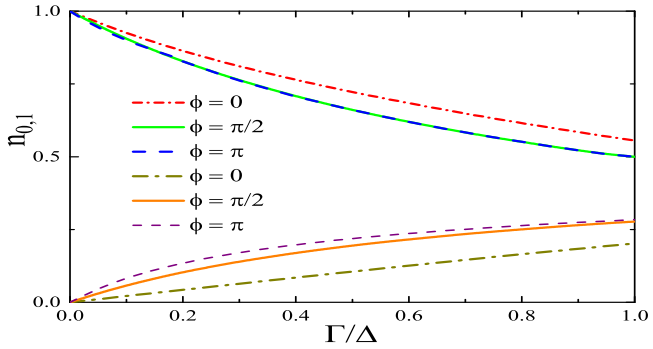

FIG. 1: (Color online) The dependence of n_0 and n_1 versus the impurity level width Γ for different values of ϕ (phase ϕ characterizes the impurity location $\mathbf{R}_{\rm imp}$ relative to the charge-density wave). For calculations $\epsilon_0 = 0.2\Gamma$ was chosen. All curves for n_1 start from 1 at $\Gamma = 0$, and decrease when Γ grows. The curves for n_0 start from zero at $\Gamma = 0$, and grow when Γ grows.

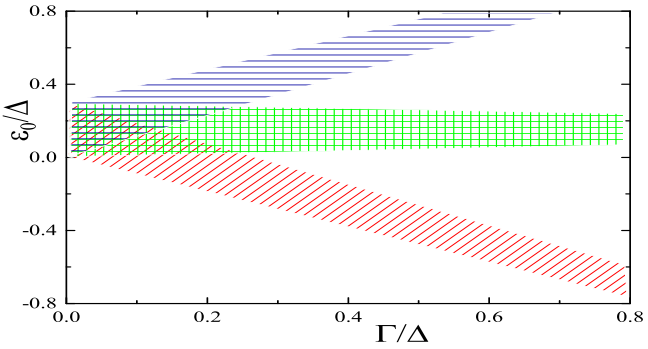

FIG. 2: (Color online) The phase diagram of a single impurity on the plane $(\Gamma/\Delta, \epsilon_0/\Delta)$. The value of U is equal to 0.3Δ The hatched areas correspond to the magnetic phase. The difference between the three hatched areas is the value of phase ϕ, which depends on the location of the impurity relative to the density wave. Horizontally hatched area (blue) represents the magnetic phase for $\phi = 0$. Crisscrossed area (green) represents the magnetic phase for $\phi = \pi/2$. The area hatched by slanted (red) lines represents the magnetic phase for $\phi = \pi$.

E. Perturbation theory

In this subsection we calculate first-order correction to the energy of $|N_\uparrow, N_\downarrow\rangle$ induced by small, but finite U. It is given by the following matrix element:

$$\Delta E = U \langle N_\uparrow, N_\downarrow | \, d_\uparrow^\dagger d_\uparrow d_\downarrow^\dagger d_\downarrow \, | N_\uparrow, N_\downarrow \rangle = U \langle n_\uparrow \rangle \langle n_\downarrow \rangle. \quad (34)$$

Since the non-perturbed Hamiltonian does not couple spin projections, the latter matrix element factorizes into a product $\langle n_\uparrow \rangle \langle n_\downarrow \rangle$, which can be evaluated easily:

$$\Delta_0 E = U n_0^2 \quad \text{for} \quad N = 0, S_z = 0, \quad (35)$$
$$\Delta_1 E = U n_1 n_0 + U n_0^2 \quad \text{for} \quad N = 1, S_z = \pm 1/2, \quad (36)$$
$$\Delta_2 E = U (n_1 + n_0)^2 \quad \text{for} \quad N = 2, S_z = 0, \quad (37)$$

where $\Delta_N E$ is the correction for the state with N electrons on the bound state. Of the three possibilities presented by Eqs. (35), (36), and (37), only $N = 1$ case corresponds to a magnetic state with non-zero spin. This state becomes the ground state if its energy $E_0 + \Delta_1 E$ is lower than both the energy $2E_0 + \Delta_2 E$ of the state with two electrons bound to the impurity, and the energy $\Delta_0 E$ for the state with zero electrons at the bound state. Therefore, the ground state is magnetic if

$$-U n_1^2 - U n_0 n_1 < E_0 < -U n_0 n_1. \quad (38)$$

For large $\Delta \gg \epsilon_0, \Gamma$ the latter condition is equivalent to:

$$U > \epsilon_0 + \Gamma \cos\phi > 0. \quad (39)$$

Equation (38) allows us to map numerically the phase diagram of the impurity.

The phase diagrams on the plane $(\Gamma/\Delta, \epsilon_0/\Delta)$ for different ϕ are presented in Fig. 2. The value of ϕ affects the details of the phase diagram, however, the magnetic phase exist for any ϕ.

This phase diagram is valid as long as the perturbation theory is justified. One can use the perturbation theory if the bound state energy E_0 lies sufficiently far from the edges of the continuous spectrum. Thus, for small U our phase diagram is valid even for large $\epsilon_0, \Gamma \lesssim \Delta$.

In Fig. 3 the phase diagram of a single impurity is shown on a different plane. This time, the horizontal axis represents ϕ, the vertical axis – interaction parameter U/Γ. The magnetic phase corresponds to the colored (yellow) area. It is easy to see that, if $|\epsilon_0| < \Gamma$, then for any non-zero value of U there is finite interval of ϕ, where the impurity is magnetic. For relatively small interaction $U \ll \sqrt{\Gamma^2 - \epsilon_0^2}$ the width of such an interval is determined by the following formula

$$\delta\phi_U = \frac{2U}{\sqrt{\Gamma^2 - \epsilon_0^2}}. \quad (40)$$

If the impurities are randomly distributed along the CDW then even weak repulsion can magnetize at least part of them. In the next section we will discuss how this affects the experimentally observed quantities.

IV. THERMODYNAMIC PROPERTIES OF AN IMPURITY ENSEMBLE

In the previous section we learned that a weakly interacting impurity in a CDW material may have magnetic ground state. In this section we will demonstrate that in a system with finite concentration of such impurities the magnetic susceptibility diverges at zero temperature, while the heat capacity at finite temperature demonstrates pronounced peak at weak magnetic field.

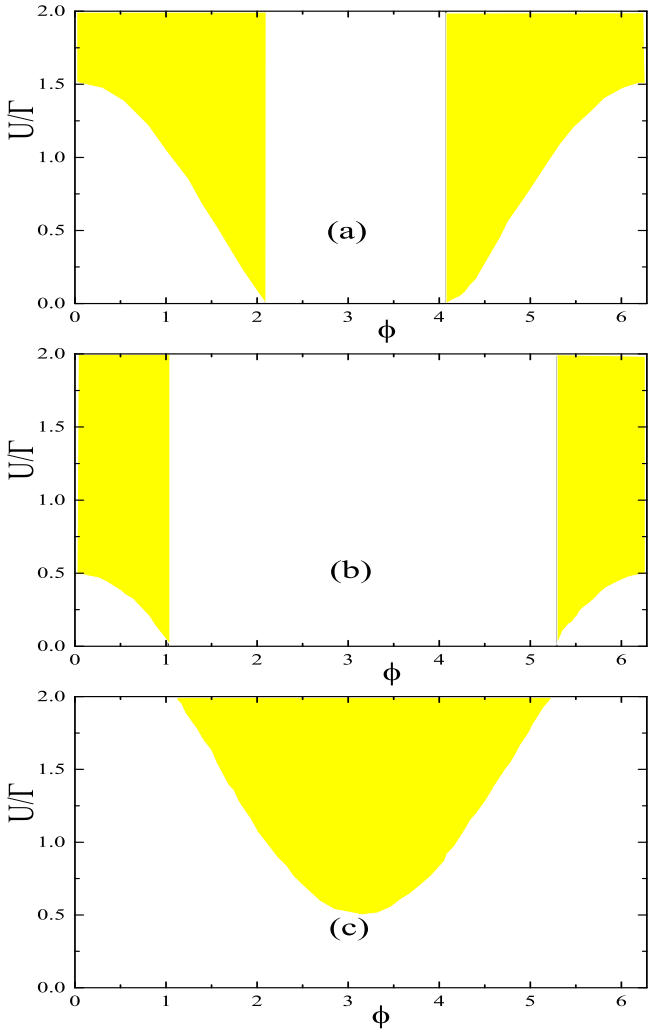

FIG. 3: (Color online) The phase diagrams of the impurity for three different value of the on-site potential ϵ_0. Vertical axis is the Coulomb repulsion U, the horizontal axis is ϕ. Colored (yellow) area shows the magnetic phase. Panel (a) corresponds to $\epsilon_0 = -0.5\Gamma$, panel (b) corresponds to $\epsilon_0 = 0.5\Gamma$, panel (c) corresponds to $\epsilon_0 = 1.5\Gamma$.

A. Susceptibility of a single impurity

We start our analysis with calculation of the partition function of a single impurity placed in magnetic field. Only $|N_\uparrow, N_\downarrow\rangle$ states contribute to the thermodynamic properties at low temperature and magnetic field. Their energies are:

$$\epsilon_1 = Un_0^2, \tag{41}$$

$$\epsilon_{2,3} = E_0 + Un_0(n_1 + n_0) \pm h, \tag{42}$$

$$\epsilon_4 = 2E_0 + U(n_1 + n_0)^2, \tag{43}$$

where ϵ_1 is the energy of the state with zero localized electrons on the impurity. This energy is determined by Coulomb repulsion Un_0^2 between bulk electrons tunneled to the impurity site. Energies $\epsilon_{2,3}$ correspond to the states with one localized electron. They have finite Zeeman energy $h_{2,3} = \pm\mu_B B$. When there are two electrons on the impurity site, their energy ϵ_4 is composed of two contributions: the single-electron energy $2E_0$, and the electron-electron interaction energy $U(n_0 + n_1)^2$. In the above expressions we did not include explicitly the kinetic energy of the zone electrons. Since the occupation numbers of bulk states does not change at low T and h, this portion of energy is identical for all four states $|N_\uparrow, N_\downarrow\rangle$.

The corresponding partition function is:

$$Z = \sum_{i=1}^{4} e^{-\beta\epsilon_i}, \text{ where } \beta = 1/T. \tag{44}$$

It can be used to find the free energy $F = -T\ln Z$, which, in turn, is used to calculate the magnetic susceptibility of the impurity:

$$\chi = -\frac{\partial^2 F}{\partial h^2}|_{h=0} = \frac{2\beta}{e^{\beta\overline{E}_0} + 2 + e^{-\beta(\overline{E}_0+\overline{U})}}. \tag{45}$$

Within the framework of our formalism the renormalized energies in this equation equal to:

$$\overline{E}_0 = E_0 + Un_0n_1, \tag{46}$$

$$\overline{U} = Un_1^2 \tag{47}$$

These expressions are obtained using the perturbation theory. However, Eq. (45) is more general: it captures the physics of an Anderson impurity in an insulating environment. This equation retains its physical meaning even when the perturbation theory is invalid. In this case, of course, simple perturbation theory results, Eqs. (46) and (47), must be discarded. Instead, parameters $\overline{E}_0$ and $\overline{U}$ should be derived using a more advanced technique (e.g., mean field theory).

At small T the susceptibility diverges:

$$\chi(T) \approx \frac{1}{T}, \tag{48}$$

provided that $\overline{E}_0 < 0$ and $\overline{E}_0 + \overline{U} > 0$ at the same time. Otherwise, the susceptibility vanishes at $T = 0$.

B. Susceptibility of the impurity ensemble

Of course, in a sample numerous impurities exist. If the impurities are not too dense, they can be treated independently. To study a macroscopic sample in the diluted limit single-impurity properties must be averaged over an ensemble of impurities.

To perform the averaging we assume that all impurities have the same values of the "internal" parameters U, Γ, and ϵ_0. The phase ϕ, on the other hand, will be treated as a random variable homogeneously distributed over the interval of $(0, 2\pi)$. This means that the locations of the impurities do not correlate with the charge-density

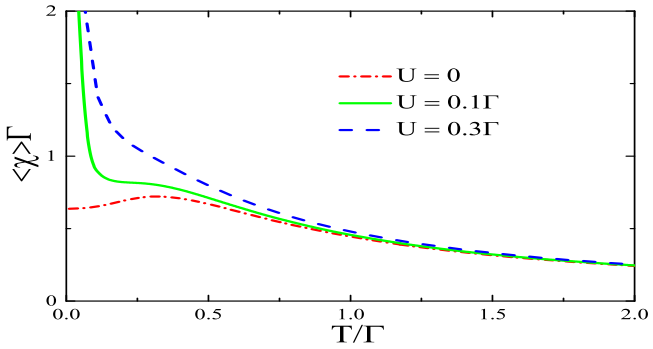

FIG. 4: (Color online) The ensemble-averaged magnetic susceptibility $\langle\chi\rangle$ versus temperature T for different values of the Coulomb repulsion U/Γ. Other parameters are: $\epsilon_0 = 0.1\Gamma$, Note that $\Gamma > \epsilon_0$. When this condition is met, the susceptibility diverges at small T for arbitrary weak U. By contrast, the ensemble of $U = 0$ impurities has finite susceptibility at $T = 0$.

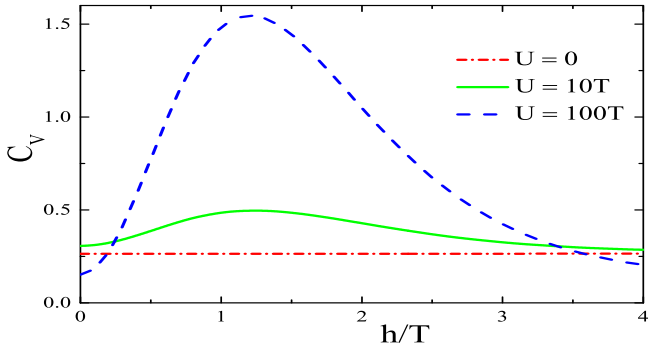

FIG. 5: (Color online) The heat capacity C_V of the impurity ensemble versus Zeeman energy h for different values of the interaction parameter U. For calculations we used $\Gamma = 50T$ and $\epsilon_0 = T$. If $U = 0$, the heat capacity is virtually field independent at small h. For non-zero U finite concentration of the magnetized impurities emerge, and C_V develops maximum at weak field $h \sim T$. We see also that the interaction U significantly enhances the weak field heat capacity.

modulations in the CDW phase, which is equivalent to weak pinning of the CDW by the impurities. (The case of strong pinning will be briefly discussed in Sec. V.)

The ensemble of this type has an interesting property: if $\Gamma > \epsilon_0$, then for any non-zero U a finite fraction of the impurities are in the magnetic state. In other words, arbitrary small interaction is sufficient to generate the divergent susceptibility of the ensemble. The results of numerical calculations illustrating this point are presented in Fig. 4. There the dependence of the ensemble-averaged magnetic susceptibility $\langle\chi\rangle$ is shown as a function of temperature for different values of the repulsion U. If there is no interaction, then $\langle\chi(T)\rangle$ is finite for any temperature. However, the susceptibility demonstrates $1/T$ divergence (the Curie's law) even for weak U. The smaller the interaction, the lower the temperature at which the susceptibility starts to diverge.

C. Ensemble heat capacity

Besides the susceptibility, the heat capacity of o-TaS_3 as a function of temperature and magnetic field has been measured[1,9]. It is not difficult to extend the formalism of the previous subsection for calculation of the impurity ensemble heat capacity C_V. It equals to:

$$C_V(T,h) = -T\frac{\partial^2\langle F(T,h)\rangle}{\partial T^2}, \qquad (49)$$

where $\langle F\rangle$ denotes the ensemble-averaged free energy.

The dependence of C_V on Zeeman energy h for fixed temperature is presented in Fig. 5. As we can see, if $U = 0$, the heat capacity is quite insensitive to weak magnetic field. However, for non-zero interaction C_V becomes a non-monotonous function of the magnetic field, with maximum near $h \sim T$. The maximum is associated with the contributions of those impurities on which exactly one electron resides. Since the number of such impurities in the ensemble grows when U increases, the weak field heat capacity may be significantly enhanced by the interaction, as one can see from the graphs in Fig. 5

V. DISCUSSION

A. Comparison to experiment

Above we proposed a mechanism describing the emergence of localized magnetic momenta in a material with CDW order. Within the framework of our model we were able to show that the magnetic susceptibility of the system diverges at low T. This behavior resembles the phenomenology observed in experiments on o-TaS_3, Ref. 1, and YTe_3 and $LaTe_3$, Ref. 4,5. Specifically, the susceptibility of o-TaS_3 is virtually temperature-independent for a broad range of temperatures, both above and below its CDW transition temperature of $T_{CDW} = 218\,K$. However, below $\sim$60 K the susceptibility diverges as $T \to 0$. Ref. 1 explored the details of this divergence.

Non-magnetic tritellurides YTe_3 and $LaTe_3$ demonstrated diamagnetic susceptibility with weak temperature dependence[4,5]. However, below $\sim$ 10 K divergent paramagnetic contribution appears, see Fig. 6.1 of Ref. 4. While that contribution has been dismissed as being due to contamination by magnetic atoms, no experimental proof to this statement has been offered. Obvious similarity between the behavior of the quasi-two-dimensional and quasi-one-dimensional materials suggests that, beside contamination, other options must not be dismissed off hand. Clearly, the susceptibility divergence of both TaS_3 and the tritellurides is in agreement with the conclusions of our study.

Another interesting experimental feature of o-TaS_3 is

the sensitivity of its heat capacity to low magnetic field. In Ref. 2 it has been reported that at $T = 0.1\,\mathrm{K}$ the field-sensitive contribution to C_V passes through maximum when the magnetic field B is equal to $0.1\,\mathrm{T}$. Such a magnetic field corresponds to the Zeeman energy $h = \mu_B B = 0.065\,\mathrm{K}$. This is consistent with the heat capacity behavior presented in our Fig. 5: if $U > 0$, then $C_\mathrm{V}(h)$ has a pronounced maximum at $h \sim T$.

B. Spin-spin interaction

Our model qualitatively reproduces both the susceptibility divergence and the sensitivity of the heat capacity to the magnetic field, yet, there are obvious discrepancies with the data. On experiment the susceptibility diverged with fractional exponent; the heat capacity demonstrated hysteresis when magnetic field was varied.[1,2]. To describe these phenomena the model of non-interacting impurities is insufficient. It is likely that interaction between impurity spins must be accounted for. For example, random-exchange antiferromagnetic Heisenberg model has been mentioned in Ref. 1 as a possible low-temperature effective theory responsible for the fractional exponent in the susceptibility data. However, a study of such an interaction is beyond the scope of this paper.

C. Strength of the effective Coulomb interaction

Our investigation demonstrates that the repulsion between electrons on the impurity site U is of crucial importance for non-trivial magnetic properties of the CDW. The non-zero U is necessary to explain both the divergence of the magnetic susceptibility (see Fig. 4), and the low field peak of the heat capacity (see Fig. 5).

Given such a sensitivity to U, we would like to discuss its value. Clearly, we can give reasonable estimate for the interaction strength only when the nature of the impurities is known. If we deal with an atomic impurity, the value of U may be as high as eV or several eV due to strong localization of the atomic orbitals. For such a high value of the interaction the perturbation theory is not applicable. Instead, one should use the mean field theory to find the impurity magnetization self-consistently. As for the main conclusions of our study, they remain unchanged. However, if such high-U impurities were indeed present in the material, they might form localized magnetic momenta even in the metallic phase (provided that $\epsilon_0 < 0$) even in the metallic phase. Yet, it appears that at high temperature nothing anomalous has been reported.

On the other hand, visually examining experimental data in Fig. 1a of Ref. 1, we notice that the susceptibility of TaS_3 starts to grow below $\sim 100\,\mathrm{K}$. If we interpret this observation within the framework of our model, the following rough estimate $U \sim 100\,\mathrm{K} = 10\,\mathrm{meV}$ can be made. Such a small value of U could mean one of two things. Either (i) the effective value of U experiences strong renormalization due to, for example, hopping to the bulk, or (ii) that "the impurities" are, in fact, shallow defects due to structural imperfections.

The decreasing renormalization of U due to hopping is quite expected. However, to justify case (i) the renormalization must be very strong: about two orders of magnitude, from $\sim$eV to $\sim 10\,\mathrm{meV}$. It is not clear if this could be rationalized for a real material. However, if it is indeed possible, then our formalism may be straightforwardly applied to such a system.

Regarding case (ii), our model cannot be immediately applied to such "impurities": the hybridization Hamiltonian, Eq. (4), corresponds to a very localized impurity state, which hybridizes with the band states at $\mathbf{R} = \mathbf{R}_\mathrm{imp}$ only. However, the main conclusions of our analysis endure.

To prove the latter statement, consider the following reasoning. Let us model the crystal imperfections by spatial variation of the single-particle potential $V = V(\mathbf{R})$. It is finite near the imperfection:

$$V(\mathbf{R}) \sim V_0 < 0, \text{ if } |\mathbf{R}| < R_0, \tag{50}$$

and zero otherwise. In a gapful environment, like CDW material, if V_0 is sufficiently deep, and R_0 is sufficiently large, the imperfection may host a subgap localized state. Due to very extended wave function the effective U for such a state is low. However, for a shallow subgap state even weak U might be sufficient to push the second electron out, generating a spinful ground state. An ensemble of these states would demonstrate both the divergent susceptibility, and the low field peak of $C_\mathrm{V}(h)$.

D. Strong versus weak pinning

When we averaged over the impurity ensemble in subsection IV B, we assumed that the positions of impurities and the order parameter phase ϕ are not correlated. This assumption is equivalent to homogeneous distribution of ϕ in the impurity ensemble.

However, in general, the CDW pinning introduces the correlation between the impurity position and the phase ϕ. Indeed, an impurity and the CDW interact. The corresponding pinning energy is a periodic function of ϕ. An impurity ensemble introduces local distortions to the CDW to minimize the pinning energy at the expense of the CDW elastic energy. For weakly pinned CDW this distortion is weak. In this situation the correlation between impurity positions and ϕ may be neglected.

In the opposite limit of strong pinning a given impurity strongly distorts the CDW to choose a particular value of ϕ, which minimizes the pinning energy function. In such a regime the assumption of homogeneous distribution of ϕ is, clearly, invalid. Instead, a distribution function would concentrate around a particular value (or values) of ϕ. This, however, does not affect the major conclusions of our study. Specifically, both the divergence of the susceptibility and the low field maximum

of the heat capacity are consequences of the impurities hosting spins. To generate at least some amount of the spinful impurities the ensemble we have introduced in subsection IV B requires arbitrary weak U. For different distribution function it may be necessary for U to exceed some critical strength U_c. If $U > U_c$, then both divergent susceptibility and non-monotonous field-dependent heat capacity should be expected.

E. Mechanism of Vakhitov et al.

A possible theoretical mechanism explaining generation of the magnetic moments in CDW state has been proposed in Ref. 8 by Vakhitov and co-authors. In that reference a strongly anisotropic quasi-one-dimensional (Q1D) metal interacting with phonon mode has been studied. The metal undergoes the Peierls transition at some finite temperature. It was demonstrated that, under suitable conditions, an impurity introduced into such a system traps an unpaired electron. These impurities, randomly scattered over the sample, are responsible for the low-temperature susceptibility enhancement.

While several basic ingredients of the model of Ref. 8 are similar to the assumptions of the present paper, there is an important distinction: the proposal of Ref. 8 relies heavily on the bosonization of one-dimensional electrons. As such, it can be applied to study of Q1D systems, like o-TaS_3 and blue bronze $Rb_{0.3}MoO_3$. However, non-magnetic tritellurides $LaTe_3$ and YTe_3 are quasi-two-dimensional. Thus, it appears important to develop an alternative mechanism, operational beyond Q1D realm. Our formalism relies not on the bosonization, but rather on the mean field theory for the Frölich Hamiltonian. The mean field approach may be used for quasi-two-dimensional, three-dimensional and, with certain care[10], even for Q1D systems. Consequently, our mechanism has a much wider applicability range.

VI. CONCLUSIONS

In conclusion, we have proposed a possible mechanism responsible for the generation of the localized magnetic moments in a material with CDW. Its main idea is quite generic: for an Anderson impurity in an insulating environment one can always find a parameter range where the impurity hosts a single electron spin. Using the perturbation theory in the impurity interaction strength U, we mapped the zero-temperature phase diagram of a single impurity. It consists of magnetic and non-magnetic phases. The presence of the magnetic phase can affect the thermodynamic properties of a diluted ensemble of such impurities. It was determined that the ensemble's susceptibility diverges at low temperature, and the heat capacity demonstrates marked dependence on weak magnetic field. Both theoretical findings are consistent with the experimental observations in some CDW materials.

The mechanism is fairly robust in the sense that the nature of the impurity and some other details are not very important. While our Hamiltonian described a point-like impurity, an extended shallow level bound to a defect may be considered instead. At the same time, the mechanism is not universal: if the ensemble parameters lie outside the relevant region, no localized magnetic moments appear, and the material has trivial magnetic properties.

Acknowledgments

This work was partly supported by the Russian Foundation for Basic Research (projects Nos. 14-02-00276, 12-02-00339). The authors would like to thank S. Artemenko, S. Zaitsev-Zotov, D. Shapiro, and other participants of the condensed matter seminar of Institute of Radio-engineering and Electronics RAS for useful comments and suggestions.

[1] K. Biljakovic, M. Miljak, D. Staresinic, J. C. Lasjaunias, P.Monceau, H. Berger and F. Levy, Europhys. Lett. **62**, 554, (2003).
[2] J. C. Lasjaunias, K. Biljakovic, S. Sahling, P. Monseau, J. Phys. IV France **131**, 193 (2005).
[3] J.C. Lasjaunias, S. Sahling, K. Biljakovic, P. Monseau, J. Marcus, J. Magn. Magn. Mater. **290-291**, 989 (2005).
[4] N. Ru, Charge density wave formation in rare-earth tritellurides, PhD thesis, Stanford University, (2008).
[5] N. Ru, J.-H. Chu, I. R. Fisher, Phys. Rev. B **78**, 012410 (2008).
[6] J.-I. Okamoto, C.J. Arguello, E.P. Rosenthal, A.N. Pasupathy, A.J. Millis, arXiv:1405.5561 (unpublished).
[7] A.V. Rozhkov, Int. J. Mod. Phys. B **12**, 3457 (1998).
[8] S. N. Artemenko, S. V. Remizov, D. S. Shapiro, R. R. Vakhitov, Physica B **404**, 447 (2009).
[9] J. C. Lasjaunias, K. Biljakovic, S. Sahling, P. Monseau, J. Phys. IV France **131**, 193 (2005).
[10] A.V. Rozhkov, Solid State Phenom. **152-153**, 591 (2009). Phys. Rev. B **85**, 045106, (2012)